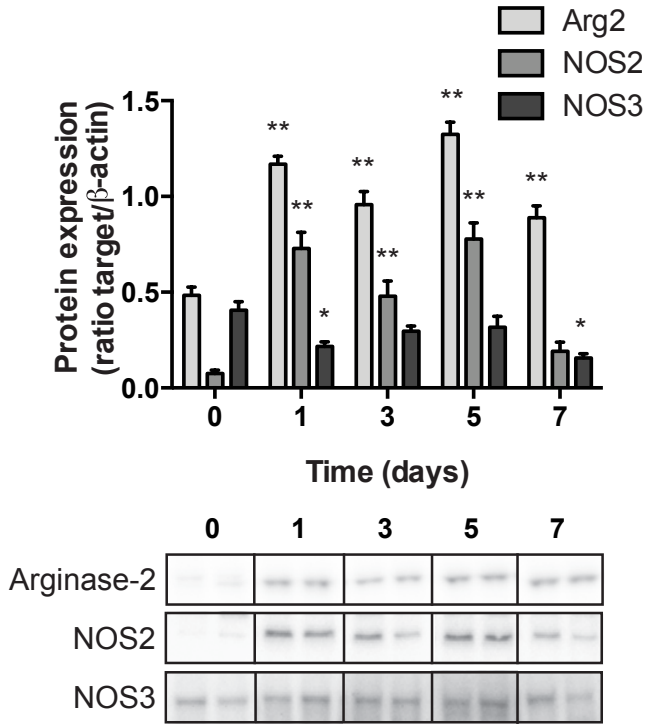

Supplemental Figure 1. Increased expression of Arginase and NOS during wound closure Wounds from wild-type mice (n=4) were harvested at days 1, 3, 5, 7, lysed and Western blotted for Arginase-2, NOS2 and NOS3 protein. The bar graph shows the ratio of the protein of interest against β-actin (au ± SEM) control with a representative Western blot below.

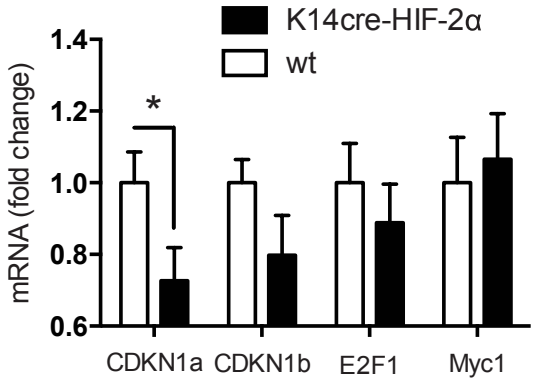

Supplemental Figure 2. C-Myc target gene expression
Basal expression of c-myc target genes in skin samples from k14cre-HIF2α or wildtype control mice. QPCR analysis (fold change, mean ± SEM) for CDKN1a, CDKN1b, E2F1 and c-myc.

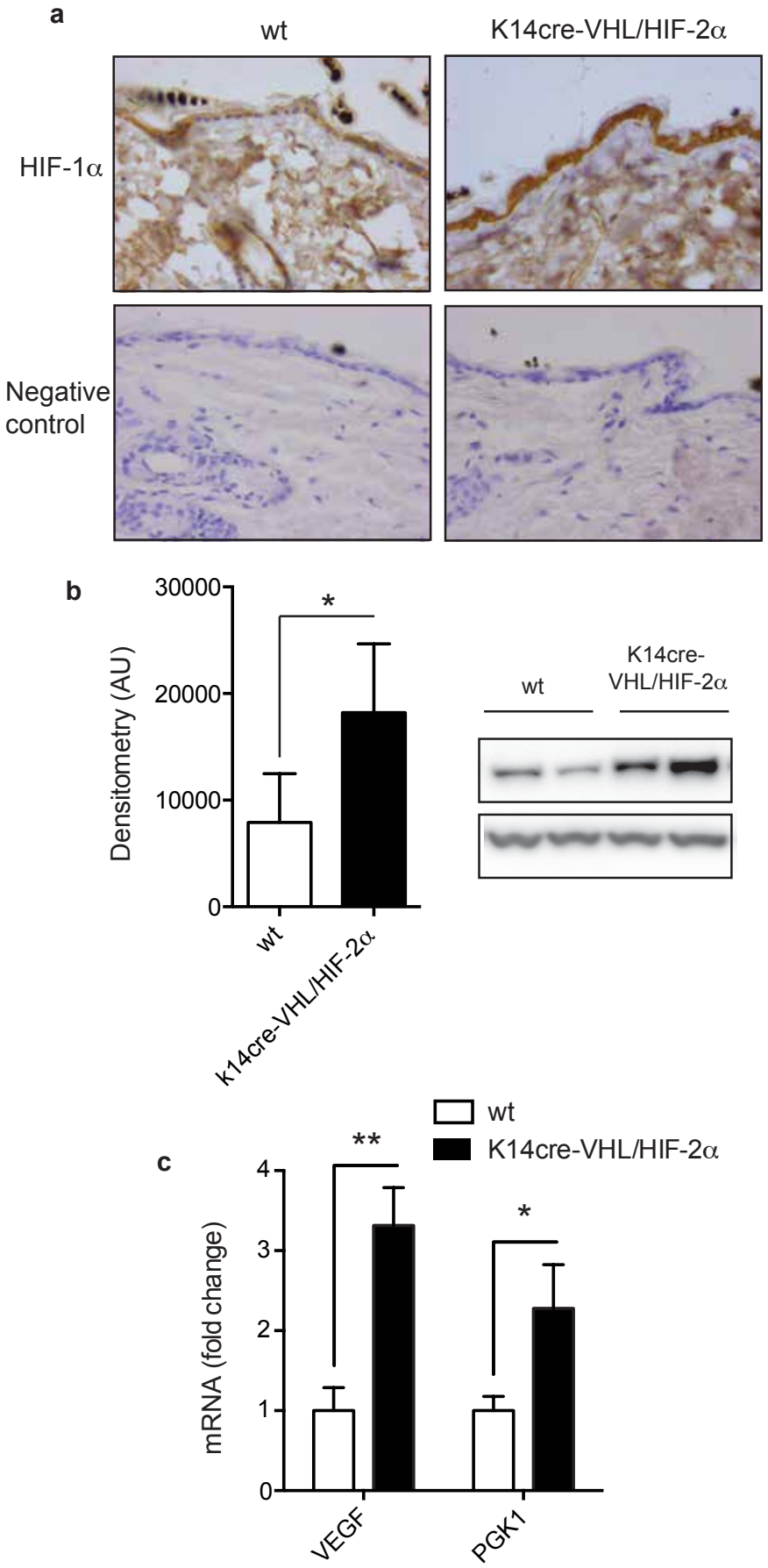

Supplemental Figure 3. Increased epidermal HIF-1α stability in K14cre-VHL/HIF-2α mouse. (a) Representative photomicrographs showing HIF-1α immunostaining on skin sections from K14cre-VHL/HIF-2α and wildtype controls. Negative controls are included below. (b) Western blot analysis for HIF-1α stability in skin lysates from K14cre-VHL/HIF-2α and wildtype controls

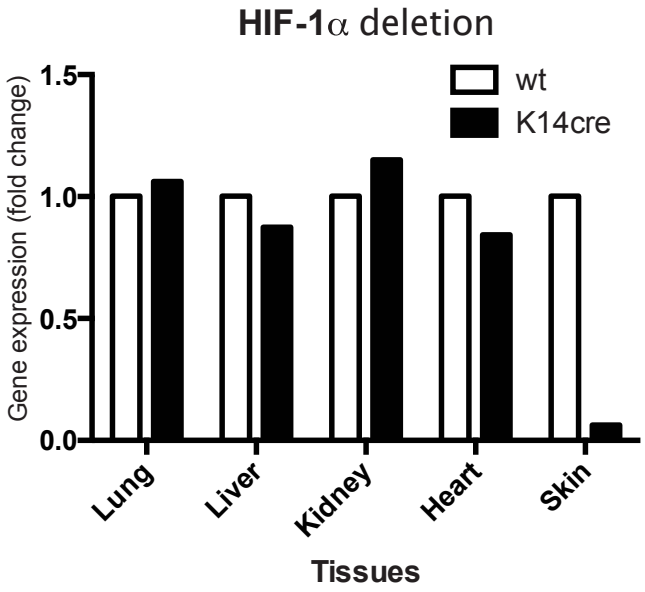

Supplemental Figure 4. K14cre deletion efficiency and tissue specificity. Taqman qPCR analysis shows the K14cre mutant to be very efficient in the deletion of HIF-1α and very specific compared to the other tissues analyzed. Data in bar graph from one experiment shown as fold change in gene expression.